The Aeronautical Journal (2022), **126**, pp. 1801–1814
doi:10.1017/aer.2022.21

REGULAR PAPER

Research and modeling of force fighting equalisation for aircraft rudder's triple active actuation system

D.W. Li[1,2], M.X. Lin[1,*] and L. Tian[3]

[1]National Demonstration Center for Experimental Mechanical Engineering Education (Shandong University), Key Laboratory of High-efficiency and Clean Mechanical Manufacture of Ministry of Education, School of Mechanical Engineering, Shandong University, Jinan, China, [2]Aviation Industry Corporation of China, AVIC XI'AN Aircraft Industry (Group) Company LTD. Xi'an, China and [3]QINGAN Co., LTD. Xi'an, China
*Corresponding author. Email: mxlin@sdu.edu.cn

Received: 4 November 2021; **Revised:** 16 January 2022; **Accepted:** 24 January 2022

Keywords: Force fighting; Redundant actuation system; Flight actuation system; Control law; Electronic-hydrostatic actuator (EHA)

Abstract

This paper presents a new approach to force fighting equalisation in a redundant active-active-active rudder actuation system that is used for the primary flight control system of a turboprop regional aircraft. The related coupled problem of force fighting scenario, and the hydraulic architecture of electronic-hydrostatic actuator (EHA) are analysed, the mathematical model of the EHA system is built. The virtual test bench is designed to evaluate the performance of the force fighting equalisation strategy. The proposed methodology is tested on an iron bird test rig. The physical experiment shows that the fighting force is minimised under all flight conditions, meets the low cost requirement and can be a very reliable system. The proposed methodology can be applied to other types of aircraft' flight actuation systems.

Nomenclature

ACE	actuator control electronics
ACM	actuator control module
Cmd.	command
DP	differential pressure
EHA	electronic-hydrostatic actuator
EMF	electromotive force
FCC	primary flight control computer
FCM	flight control module
MCE	motor control electronics
P-Q	pressure and flow
PID	proportion integral differential

1.0 Introduction

The transmission of signals in mechanical form offers relatively good reliability, which often makes the use of the redundant channel unnecessary. With the increasing advantage of electrical signals, it is becoming more and more tempting to remove auxiliary actuators. It even becomes possible to eliminate the mechanical information chain altogether if all its functions can be performed by electrically signaling the primary actuators. This leads to the invention of the fly-by-wire solution, where the primary hydro-mechanical actuator is replaced by a hydraulic actuator [1, 2]. Nowadays, multiple servo actuators are

commonly used in the primary flight control system of aircraft. This is because in active-active mode, the output displacement of each actuator is not strictly consistent. Therefore, one actuator drives another actuator, so that multiple actuators hold each other back, resulting in a force fighting scenario. Force fighting is defined as the difference between the forces produced by two or more actuators in the same flight control surface.

For reasons of safety and availability, the primary flight control surfaces (rudders, ailerons, elevators, etc.) are moved by a combination of two or more actuators, either in an active-passive configuration or in an active-active configuration. A turboprop regional aircraft's rudder is moved by three EHAs with triple active control mode. In the active-passive-passive configuration, a single actuator has the ability to drive the rudder surface. The weight and volume of the actuator are comparable large, but it does not involve the problem of force fighting. While for the active-active-active configuration, the size and weight of each actuator is relatively small, the actuators share their workload equally and can therefore be sized accordingly, but they can be influenced by the dissimilar output force of the actuators, resulting in a force fighting scenario, leading to unacceptable fatigue damage to the aircraft structure. If the flight actuation system is operating in all active mode, the controller must control the position of the surface and minimise force fighting.

In previous literature, Carlton Y. Ma utilised a pressure flow control servo-valve and an electronic auto-rigging to minimise the force fighting between two or more channels. The servo actuator may generate null difference because of thermal drift during flight, for large temperature variations at high altitude. After auto-rigging, the force fighting that is caused by the additional null difference is minimised by the smooth pressure gain of the P-Q valve [3].

Olaf Cochoy et al. proposed a hybrid actuator scheme, in which an electro-hydraulic servo actuator (EHSA) and an electromechanical actuator (EMA) operate on the same control surface. And the authors state the most effective technology is to feed back all three error representing signals, position differences of the actuators, the difference between the velocities and the occurring fighting force at the same time. Maximum force fighting between all actuators is decreased from 500% to 7% of the stall load in active-active mode [4]. Vojislav Soronda presents a system and solution of reducing a force fighting between hydraulic actuators which are coupled to a single flight control surface. First, differential pressure across each hydraulic actuator is detected. Second, using a plurality of user interface position sensors, the position of a user interface is detected. Third, using one or more position sensors, flight control surface position is detected. The sensed flight control surface position, user interface positions, and differential pressures are used to create a plurality of substantially equal actuator commands [5].

Lijian Wang et al. propose in the position control loops, to add equalisation offsets based on the integral of the force difference between the actuators to achieve static force equalisation, and by forcing the two actuators to follow the same trajectory to achieve the dynamic force equalisation. A path generator is introduced to generate the required acceleration, position, and velocity from the position set point with real reproduction of the actuators' power limitation. Using feed forward actions to compensate the invariant and major effects such as electro-mechanical actuator inertial torque and servo-hydraulic actuators functional flow. By this approach, tracking errors are greatly reduced without reducing robustness [6].

Ur Rehman Waheed et al. present four position synchronisation methods. The first one uses proportion integral differential (PID) controller to improve load rejection performance, and self-tuning Fuzzy PI controller to control position loop dynamics. The second method uses a PID controller to balance position loop dynamics. The third and fourth strategies use PID for pre-compensators and position loop dynamics to equalise force dynamics [7].

Tobias Röben et al. propose electro-hydrostatic, electro-mechanic and servo-hydraulic to build a hybrid all-active actuation system. Using a feed-forward control method and a conventional PI controller, which addresses remaining static force fight, to reduce force fighting during acceleration or deceleration process. A control electronic is developed for generic use with each single actuator, which includes kinematic conversion, position control, force fighting control and safety monitoring functions [8].

Additionally, other different control algorithms are invented to achieve force fighting equalisation of flight control actuators, such as model reference adaptive controller, feed-forward controller and

https://doi.org/10.1017/aer.2022.21 Published online by Cambridge University Press

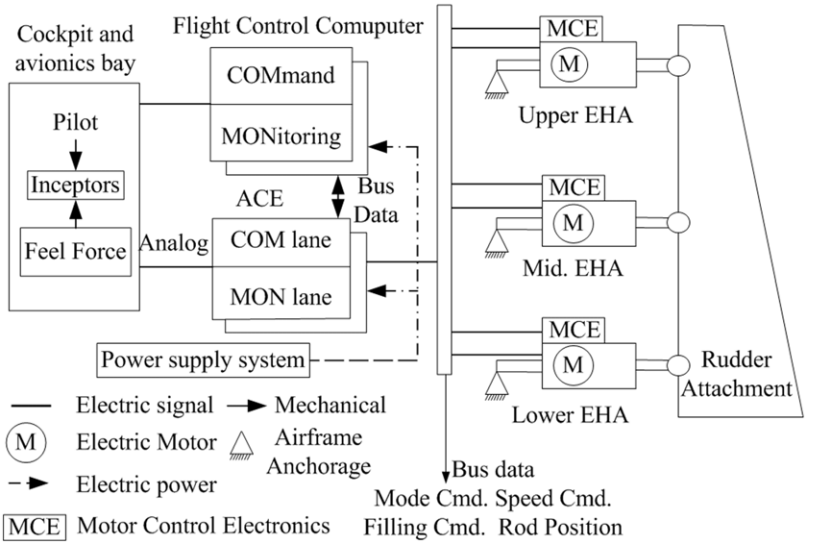

Figure 1. *Rudder control system scheme.*

feedback controller, fractional order PID (FOPID) controllers, fault-tolerant synchronisation controller, feedback loop designed as an optimal linear quadratic output regulator (LQR) and a feed-forward controller based on a general regression neural network (GRNN) [9–12].

In order to solve the force fighting problem of the rudder actuating system for a certain type of aircraft's active-active-active operational mode, taking into account the reliability, maturity, safety and cost of the technical solution, this paper uses position feedback and differential delta pressure feedback to establish a dual closed-loop servo control, using a PI controller as an outer loop controller plus an inner loop PI controller to achieve force fighting equalisation. Through the equivalent transformation of the physical model, mechanical kinetic analysis and mathematical modeling, an accurate virtual test rig is built by the AMEsim modeling software. The simulation results and the results of the iron bird test show that the dynamic fighting force decreases significantly and can be considered as a force fighting equalisation scheme for other aircraft types.

2.0 Mathematical model of rudder redundant actuation system

2.1 Problem formulation and context

The primary flight control system of a turboprop regional aircraft mainly contains aileron, rudder, elevator and aileron, and has the functions of manual trim operation, control surface variation limitation and stall protection, etc. It adopts electrical signal transmission control and hydraulic power drive. The primary flight control system mainly consists of control stick/disc assembly, pedal assembly, flight control panel, trim control panel, deceleration control handle, primary flight control computer (FCC), actuator control electronics (ACE), control surface position sensors, spoiler actuators, elevator actuators, aileron actuators and rudder actuators, etc. Each FCC comprises a flight control module (FCM) and an actuator control module (ACM). Each FCM is equipped with control and monitoring channels; ACM and ACE have the same function, both are equipped with monitoring and control channels, but adopt different hardware configuration. The simplified architecture of a turboprop regional aircraft's rudder flight control actuation system is shown in Fig. 1.

The rudder is driven by three electronic-hydrostatic actuators (EHA). The EHAs are identical to provide the necessary system redundancy and can be installed in any of the three mounting locations.

https://doi.org/10.1017/aer.2022.21 Published online by Cambridge University Press

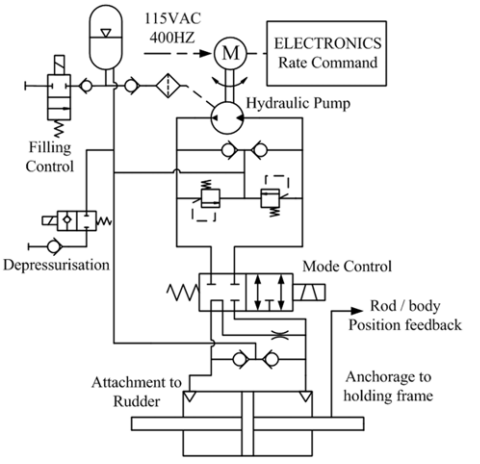

Figure 2. *Hydraulic architecture of an EHA [1].*

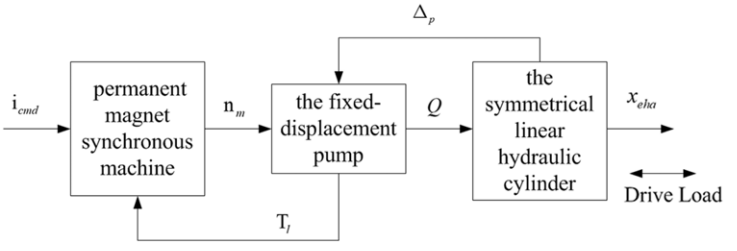

Figure 3. *EHA architecture with servo motor, fixed pump and hydraulic cylinder.*

The primary control system uses an active-active-active mode to proportionally control the EHA position from the aircraft control system commands. The EHA's input current commands control the flow of fluid to control the position and rate of the EHA. The triple active mode requires the shut-off-valve (SOV) to be activated and the supply pressure to be above a threshold pressure. The maximum rudder panel movement is reduced as the airspeed increases. Maximum rudder panel deflection is approximately around +/−8 degrees at a typical cruising altitude, +/−20 degrees on the ground.

Figure 2 shows the general structure of an EHA. It mainly consists of control and power electronics, the electric motor, the fixed displacement pump, symmetrical linear hydraulic cylinder, the re-feeding valves, pressure relief valves, solenoid valve, hydraulic restrictor, fluid filter, oleo-pneumatic accumulator and solenoid valve, etc. [13].

As shown in Fig. 3, EHA contains a permanent magnet synchronous machine (PMSM), a fixed displacement pump and a hydraulic cylinder. The movement of piston is computed by the shaft speed of a permanent magnet synchronous machine. The fixed displacement piston pump generates the flow of hydraulic fluid. By pressurising a hydraulic cylinder, the linear motion of an electro-hydrostatic actuator is achieved.

2.2 Mathematical model of PMSM

In order to build the mathematical model of electronic-hydrostatic actuator, with regards to the nonlinearities, some assumptions are made in order to obtain one linear differential equation. The maximum EHA performance (torque and speed) is defined by external load, valve gain and the supply pressure

https://doi.org/10.1017/aer.2022.21 Published online by Cambridge University Press

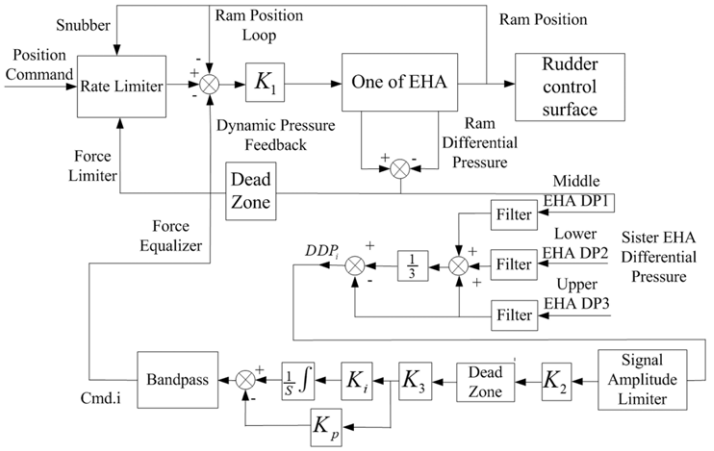

Figure 4. *Force fighting equalisation control concept scheme.*

potential. However, the electric motor's output is only limited by means of control. According to reference [14–19], the dynamic behaviour of a PMSM is mainly influenced by the characteristic winding resistance(R) and winding inductance(L), it is calculated using Equation (1) [16].

$$T_M = \frac{K_M}{R}\frac{1}{\frac{L}{R}s+1}\cdot(U - K_{EMF}\cdot\omega_M) \tag{1}$$

Where T_M is static torque of the motor shaft, U is the scalar voltage requirement as output of the MCE's control stage. The motor constant K_M is influenced by motor material and geometry. ω_M is the motor's rational speed. K_{EMF} represents the electromotive force constant.

The rotational movement of the motor shaft induces a back electromotive force (EMF) voltage into the stator coils. With its rotating mass, EMF has a lagging effect on the acceleration of the motor shaft. By neglecting the dynamic induced by these lag elements, the static motor shaft torque becomes approximately proportional to the current intake:

$$T_M \approx K_M I_M \tag{2}$$

2.3 Mathematical model of piston pump

The theoretic volume flow (Q_P) results from the motor shaft speed:

$$Q_P = \upsilon\cdot n_m = \frac{\upsilon}{2\pi}\cdot\omega_M \tag{3}$$

Where υ represents the axial piston pump displacement which determined the fluid flow, and n_m represents rotational speed of the motor.

The axial piston pump displacement υ and the rotational motor speed n_m mainly influence the piston pump's hydraulic fluid flow. The axial piston pump displacement υ, it is calculated using Equation (4) [20].

$$\upsilon = z\cdot\frac{\pi d^2}{4}D_z\tan\alpha \tag{4}$$

Where α means the swash plate inclination, (D_z, d) means other geometrical parameters of the piston pump, z means the piston numbers within the cylindrical drum.

https://doi.org/10.1017/aer.2022.21 Published online by Cambridge University Press

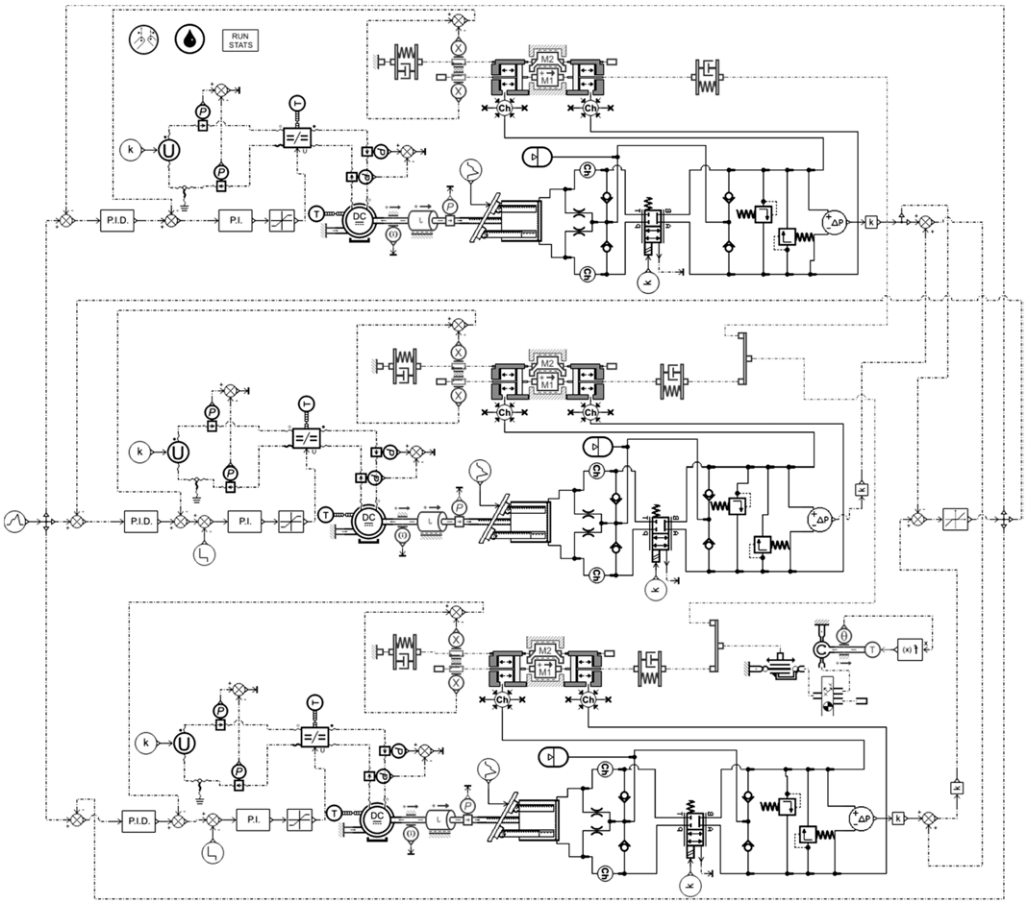

Figure 5. *The virtual test bench model.*

Considering losses of fluid compression and filling, the following theoretic volume flow equation can be modeled using Equation (5) [16].

$$Q_P = \frac{\upsilon}{2\pi}\left[1 - \frac{\Delta p}{B}\left(1 + \frac{2\upsilon_{dead}}{\upsilon}\right)\right]\omega_M \tag{5}$$

Where υ_{dead} represents the dead volume, Δp represents differential pressure within the cylinder, B stands for bulk modulus.

By formulation of a power equilibrium and introducing the load torque T_L, the mechanical coupling of pump and motor is built as follows:

$$P_M = T_L \cdot \omega_M \tag{6}$$

$$P_P = \Delta \mathrm{p}\dot{V} = \Delta \mathrm{p} \cdot Q_P \tag{7}$$

$$T_L = P_M/\omega_M = P_P/(\omega_M \eta_{mech}) = \upsilon \Delta \mathrm{p}/(2\pi \cdot \eta_{mech}) \tag{8}$$

Where P_M represents power of the motor, P_P represents power of the pump, η_{mech} represents mechanical efficiency.

https://doi.org/10.1017/aer.2022.21 Published online by Cambridge University Press

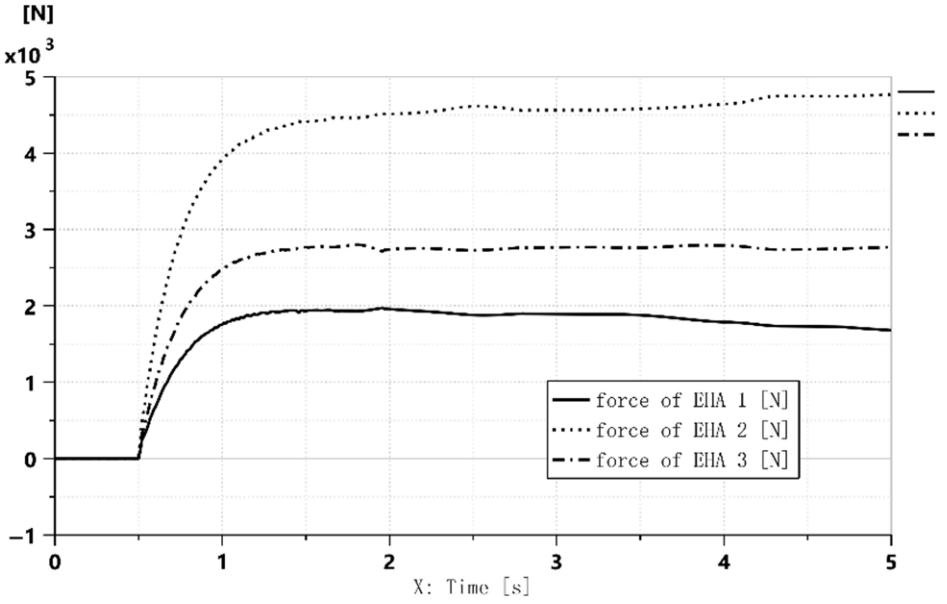

Figure 6. *Step response of the system without force fighting equalisation strategy.*

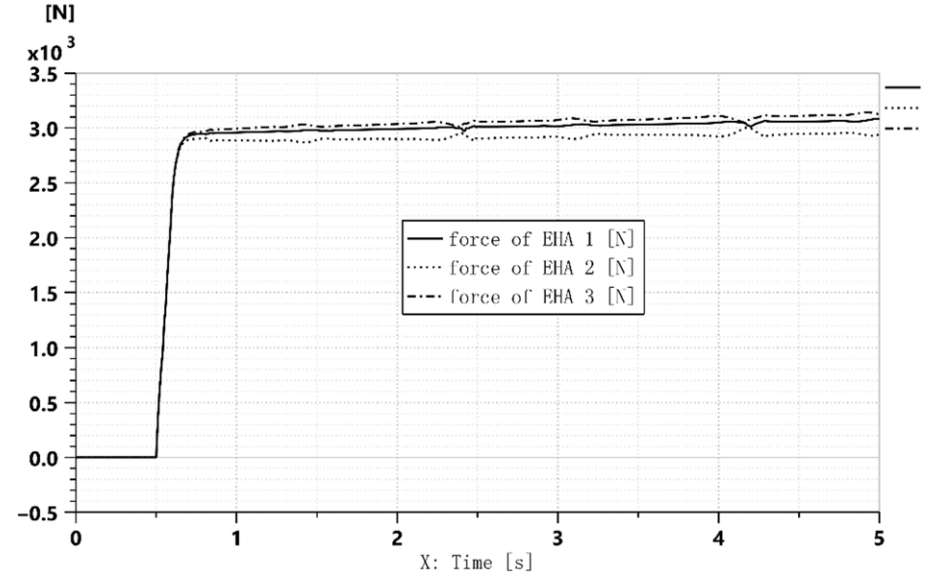

Figure 7. *Step response of the system with proposed force fighting equalisation strategy.*

Differential pressure between pump outflow and in generate the load torque, and drag torques which are caused by bearing and viscous friction between pump parts.

The drag torque T_D can be approximated by kinetic friction (d_{kin}) and static (d_{stat}), and calculated using Equation (9) [21] as follows:

$$T_D = d_{stat} \cdot sign(\omega_M) + d_{kin} \cdot \omega_M \tag{9}$$

https://doi.org/10.1017/aer.2022.21 Published online by Cambridge University Press

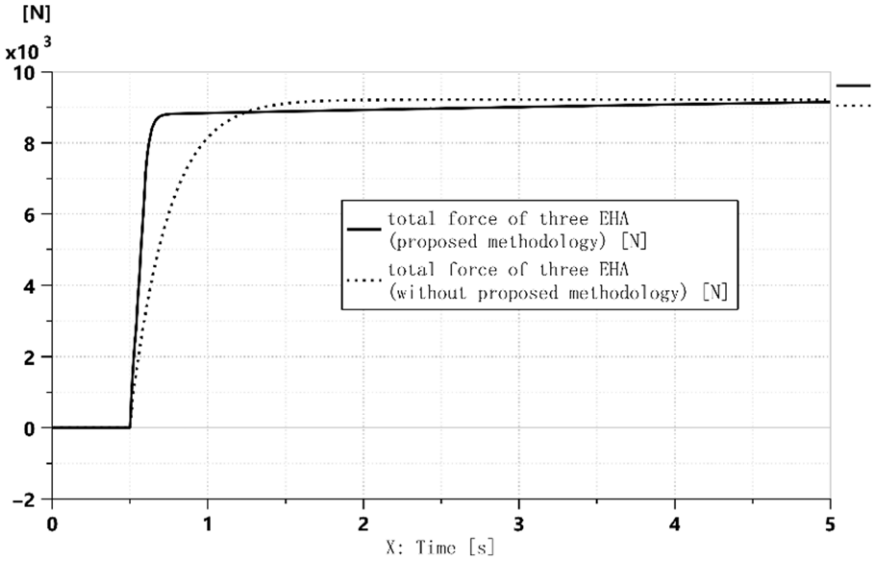

Figure 8. *Total force of the three EHAs by comparison.*

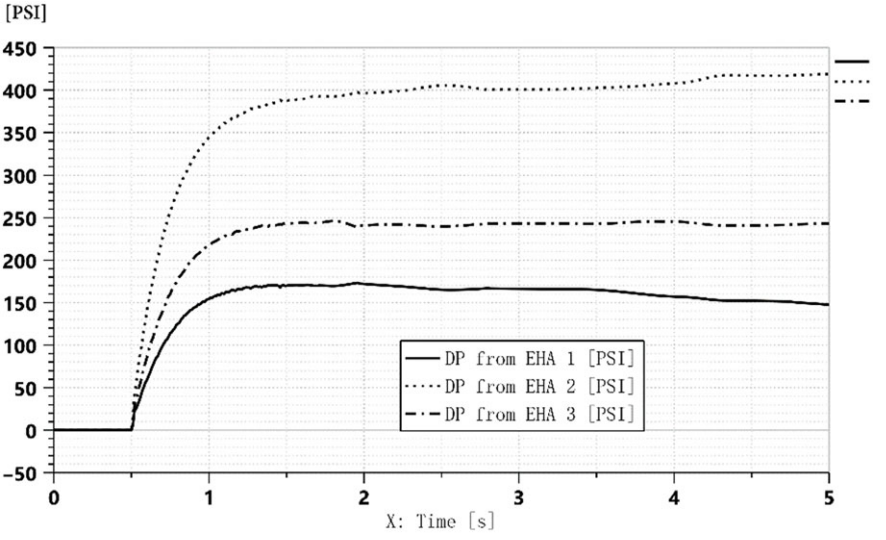

Figure 9. *Differential pressure of each EHA without proposed methodology.*

The actuator dynamic is influenced by friction effects and external cylinder load. Consideration of load torque T_L and drag torque T_D, the delivered fluid flow and the piston rod motion is determined by the operational speed ω_M:

$$J_{res}\,\dot{\omega_M} = T_M - T_D - T_L \tag{10}$$

The inertia J_{res} is composed of the rotating mass of rotor and axial piston pump.

https://doi.org/10.1017/aer.2022.21 Published online by Cambridge University Press

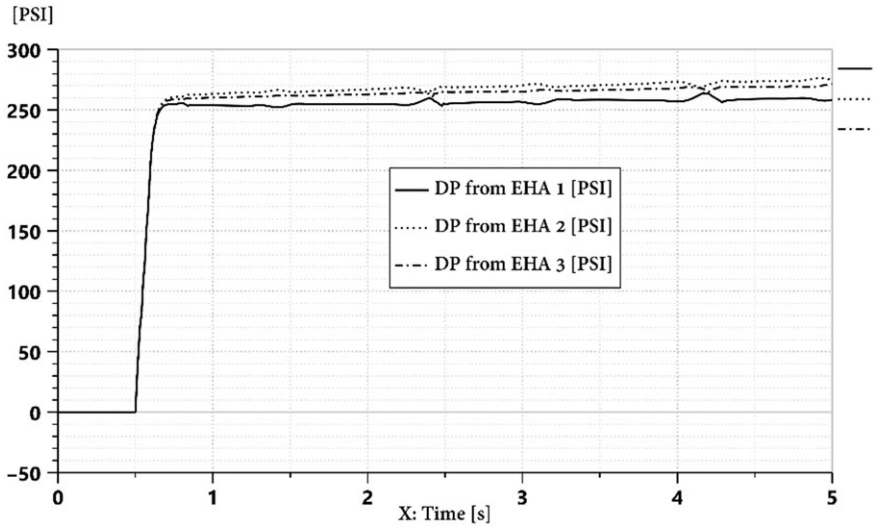

Figure 10. *Differential pressure of each EHA by proposed methodology.*

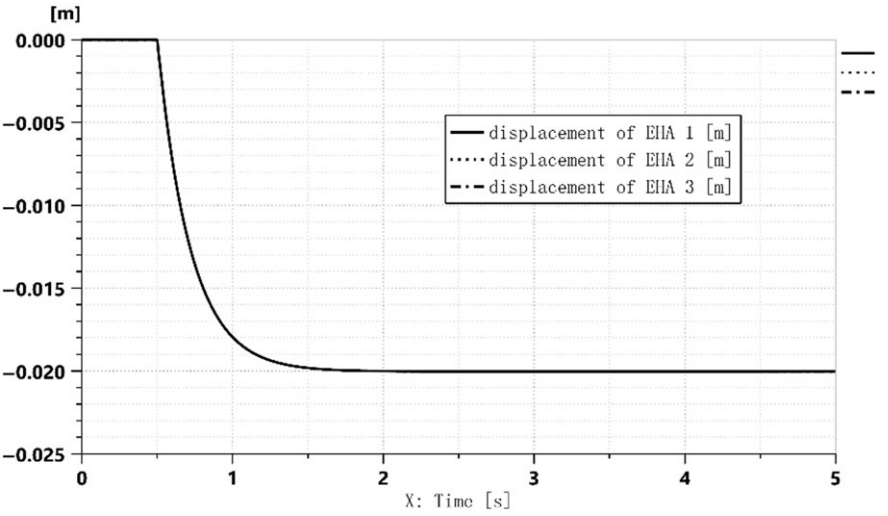

Figure 11. *Displacement of each EHA without proposed methodology.*

2.4 Mathematical model of cylinder

The hydraulic cylinder of the EHA, whose force dynamics and flow dynamics are given by the force balance equation and the continuity equation respectively:

$$Q_p = A_e\ddot{x}_{eha} + \frac{V_e}{4E_e}\dot{F}_{ext} + C_{el}F_{ext} \tag{14}$$

$$A_eF_{ext} = m_e\ddot{x}_{eha} + B_e\ddot{x}_{eha} + F_e \tag{15}$$

Where F_{ext} represents the load pressure of the hydraulic system, F_e stands for the load force acting on the actuator, Q_p stands for output flow of the hydraulic pump, A_e stands for effective area of hydraulic cylinder piston, x_{eha} stands for EHA output displacement, V_e stands for total volume of hydraulic cylinder,

https://doi.org/10.1017/aer.2022.21 Published online by Cambridge University Press

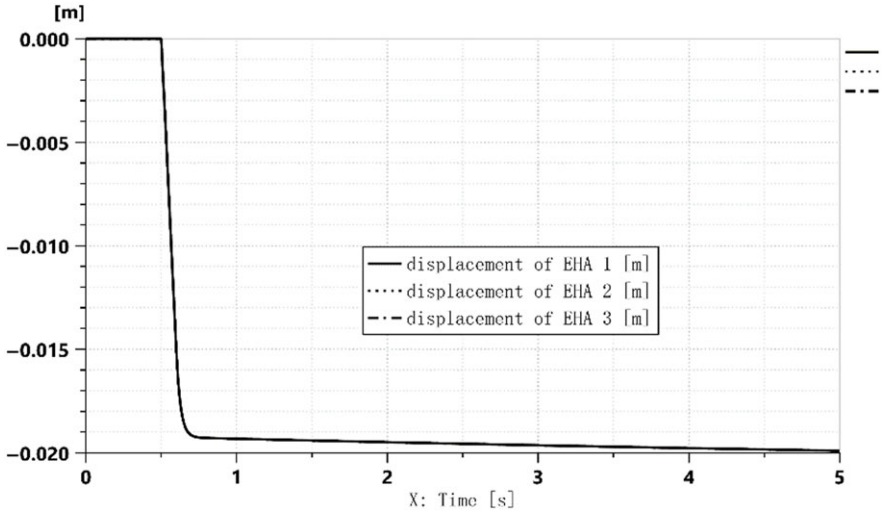

Figure 12. *Displacement of each EHA by proposed methodology.*

E_e stands for effective bulk modulus, C_{el} stands for total leakage factor, m_e stands for mass of hydraulic cylinder rod, B_e stands for viscous resistance in hydraulic cylinder.

2.5 Mathematical model of control surface

The mathematical model of the rudder of the aircraft can be constituted as coupling of mass-spring system, which is driven by the different EHA in parallel. A rigid connection is considered between EHA and control surface. The rotation angle of the control surface is very small, and are accounted for as linear movement of the control surface.

Actuator motion x_i relative to the surface position x_d results in a linear force, which drives the rudder against its own inertia, external load and friction [22–25]. Deviations between the single EHA output positions result in force fighting, which is influenced by the single channel's effective stiffness. If the direction of an output force is contrary to the other, it does not contribute to the surface positioning, but constitutes an additional load for adjacent channels. Force dynamics of aircraft rudder are given can be calculated by Equation (16) and (17):

$$F_{ei} = K(x_i - x_d) \tag{16}$$

$$F_d = \Sigma F_{ei} = m_d \ddot{x}_d + B_d \dot{x}_d + F_l + K_d x_d \tag{17}$$

Where F_{ei} represents output force of EHA number i, K represents transmission stiffness, F_d represents forces used to drive control surface, m_d represents mass of the control surface, x_d represents rudder displacement, B_d represents rudder viscous damping coefficient, F_l represents equivalent air load force, K_d represents aero elasticity.

3.0 Control strategy

In practical engineering applications, from a safety point of view, priority should be given to a mature and reliable control law. Therefore, the inertial integral balance control or PI control algorithms can be considered. Figure 4 describes the loop closures used for a turboprop regional aircraft.

Each EHA has an outer position loop, dynamic pressure feedback, force limiting, force equalisation, snubbing, and rate limiting. The actuator position loop uses quad-redundant linear variable differential

https://doi.org/10.1017/aer.2022.21 Published online by Cambridge University Press

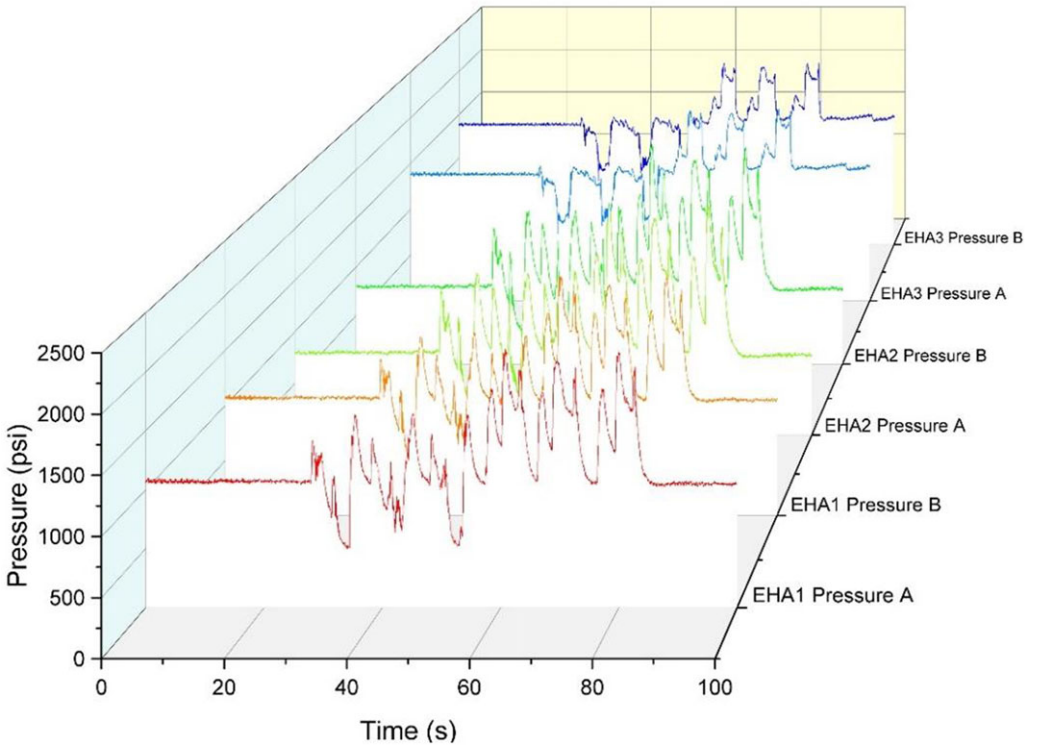

Figure 13. *Test results of each EHA's pressure curve. (A, B stands for chamber A, chamber B of each EHA)*

transformers (LVDTs) to sense EHA position and provide feedback to close the electronic loop. The pressure transducer is also used for force equalisation between EHAs on a control surface. The EHA position feedback signal is also used for position snubbing towards the end of actuator stroke and for rate limitation of the surface commands. Quad-redundant differential pressure transducers provide feedback used to dampen the load resonance mode required for the relatively high loop gain of the aircraft. The pressure transducer is also used for force limitation. Due to the relatively asymmetrical loading requirement of the aircraft, the force limiter has a dramatic effect on reducing structural weight.

In the PI control model, proportional amplification and the integral link are used. The integral link is used to reduce the steady-state error of the input response, and at the same time, make the force fighting equalisation command output more stable signal; the proportional amplification link is used to compensate for rapid pressure changes. The control mechanism of the inertial integral equalisation is the difference between the differential pressure (DP) of the EHA. The DP is used as the input of the inertia link to obtain the force balance control by tracking the system pressure difference. Dead zone link is used to avoid performing differential pressure equalisation when DP is small. The limitation link before the equalisation command is mainly used to take into account of the deviation of the rudder surface.

4.0 Virtual test bench build and physical experiment

As shown in Fig. 5, according to the actuator position closed-loop servo model and PI force fighting balance control block, a virtual test bench is built by AMEsim simulation software to evaluate the robustness of the force fighting equalisation strategy by analysing the force fighting scenario.

https://doi.org/10.1017/aer.2022.21 Published online by Cambridge University Press

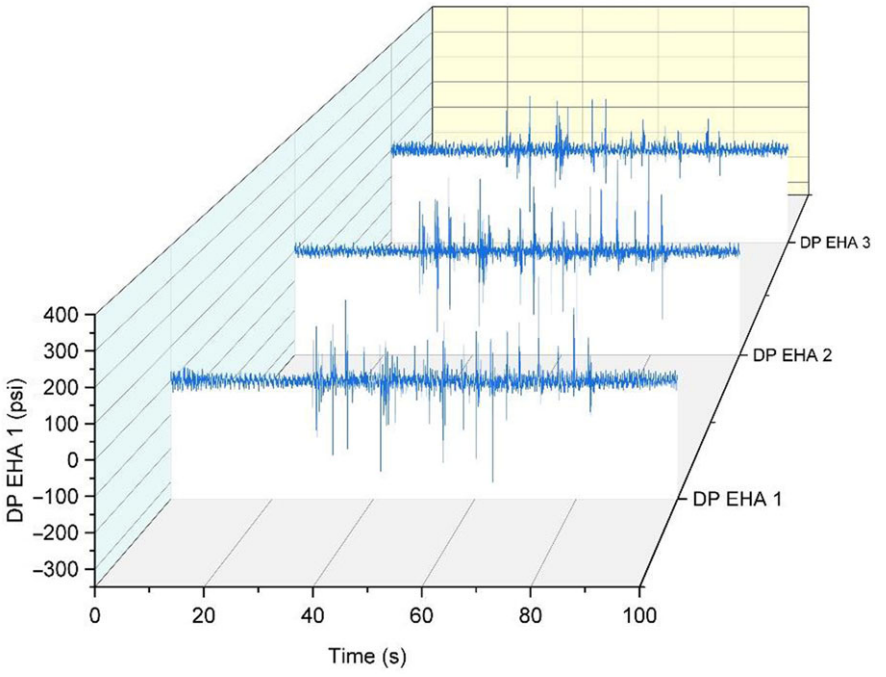

Figure 14. *Test results of each EHA's Differential pressure curve.*

A virtual simulation of the force fighting equalisation control law is performed to simulate an aircraft on the ground with aerodynamic loads, with a step signal input, to study the system response. The simulation time is set to 5 s, and the simulation step size is 0.01 s.

The simulation results without control strategy enabled are shown in Fig. 6, and the simulation results with control strategy enabled are shown in Fig. 7. In all active mode, Fig. 6 implies that the three EHA output different force, smaller output force of the other two EHAs was compensated by the other actuator. By the use of proposed methodology, Fig. 7 implies that the three EHAs output nearly the same force about 3048.68N, fighting force scenario was eliminated, and as shown in Fig. 8, the total force of three EHAs stabilise at about 9146.05N (3048.68×3), which is nearly equal to the final stabilise total force of 'without proposed methodology'. Figures 9 and 10, indicates that differential pressure of each EHA was reduced to a same curve, smaller than 50 psi by simulation. Figures 11 and 12, indicates that displacement of each EHA has a synchronisation motion, and the flight control surface has position difference. By control strategy, compared to curves of Fig. 11, curves of Fig. 12 more close to the input step signal. From the above simulation results (fighting force, differential pressure and position), it can be concluded that the fighting force between the three EHA actuators is reduced by the proposed control strategy.

Physical tests are carried out on a flight control system ground simulation test rig (iron bird), where the rudder pedal is manually operated and the step signal from the rudder pedal is converted into an electrical signal by sensors that pass through the actual flight control computer, the actuator, the electronic controller driving the actuator and the actual flight control surfaces. The test equipment collects the rudder pedal command, the equalisation command and the DP signal, so that for a single actuator it is possible to understand how the system operates in relation to the DP change equalisation control.

The curves collected through physical tests are shown in Figs. 13, 14 and 15. The raw data in Fig. 14, indicates three EHAs has a static differential pressure below about 50psi, and when EHA moves, three EHAs has a dynamic differential pressure below about 300 psi. Compare Fig. 14 (physical test) and Fig. 10 (simulation test), it indicates that physical test results have a more real and complicated

https://doi.org/10.1017/aer.2022.21 Published online by Cambridge University Press

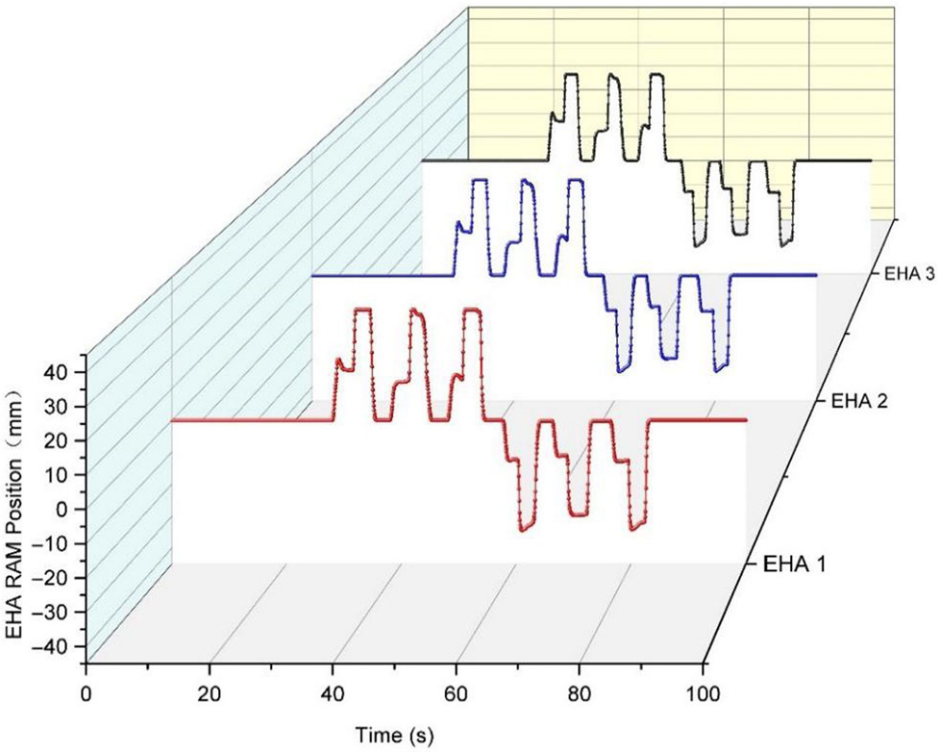

Figure 15. *Test results of each EHA's displacement.*

differential pressure fluctuation than simulation test results. To a certain type of civil aircraft, which is a twin turboprop regional aircraft with about 60 seats, its design requirement about differential pressure fluctuation is dynamic DP smaller than 500psi, static DP smaller than 100psi. From Fig. 14, it can be concluded the physical test results meet with design requirements of the research subject of this paper. Figure 15 shows that the ram position of each EHA has the same trend.

5.0 Conclusion

This paper describes the architecture of a triple active redundant actuation system for the rudder of a turboprop regional aircraft. The mathematic modeling of the actuation system is analysed and an innovative force fighting control strategy is proposed. A detailed simulation model is built in order to investigate the interaction behaviour of the different channels coupled by a control surface. Through simulation and physical experiment, it can be concluded that the main cause of force fighting in a triple active actuating system is the difference between the input commands of the residual actuator. The proposed control methodology can effectively reduce the fighting force and a uniform actuation profile can be obtained, thus meeting the design requirements of the flight control system.

Acknowledgements. This research received no specific grant from any funding agency in public, commercial or non-profit sectors.

References

[1] Maré, J-C. (2017). Aerospace actuators 2 (signal-by-wire and power-by-wire) ‖ notations and acronyms, doi: 10.1002/9781119332442, 235–243.

[2] Xue, Y. and Yao, Z.Q. A way to mitigate force-fight oscillation based on pressure and position compensation for fly-by-wire flight control systems, *Trans. Japan Soc. Aeronaut. Space Sci.*, 2020, **63**, (1), pp 1–7.

https://doi.org/10.1017/aer.2022.21 Published online by Cambridge University Press

[3] Ma, C.Y. Fly-By-Wire Dual-Dual Flight Control Actuation System, 1, 1998.
[4] Cochoy, O., Hanke, S. and Carl, U.B. Concepts for position and load control for hybrid actuation in primary flight controls, *Aerosp. Sci. Technol.*, 2007, **11**, (2–3), pp 194–201.
[5] Flight Control Surface Actuation Force Fight Mitigation System and Method. U.S. Patent No. 8,583,293 B2, 12 November 2013.
[6] Wang, L. and Mare, J.C. A force equalization controller for active/active redundant actuation system involving servo-hydraulic and electro-mechanical technologies, *Proc. Inst. Mech. Eng. G J. Aerosp. Eng.*, 2014, **228**, (G10), pp 1768–1787.
[7] Rehman, W.U., Wang, S., Wang, X. and Kamran, A. A position synchronization control for HA/EHA system, Fluid Power and Mechatronics (FPM), 2015 International Conference on IEEE, 2015.
[8] Röben, T., Stumpf, E., Weber, G. and Grom, T. An innovative all-active hybrid actuation system, *AIAA Modeling & Simulation Technologies Conference* 2015.
[9] Rehman, W.U., Wang, X., Wang, S. and Azhar, I. Motion synchronization of HA/EHA system for a large civil aircraft by using adaptive control, Guidance, Navigation & Control Conference IEEE, 2017.
[10] Rehman, W.U., Nawaz, H., Wang, S., Wang, X. and Elahi, H. Trajectory based motion synchronization in a dissimilar redundant actuation system for a large civil aircraft, 2017 29th Chinese Control And Decision Conference (CCDC), 2017.
[11] Ijaz, S., Yan, L. and Hamayun, M.T. Fractional order modeling and control of dissimilar redundant actuating system used in large passenger aircraft, *Chinese J. Aeronaut.*, 2018, **31**, pp 279–290.
[12] Li, T., Yang, T., Cao, Y., Xie, R. and Wang, X. Adaptive robust fault-tolerant synchronization control for a dual redundant hydraulic actuation system with common-mode fault, Math. Prob. Eng., 2018, **2018**, pp 1–14.
[13] Maré, J-C. "Aerospace Actuators 3 (European Commercial Aircraft and Tiltrotor Aircraft) || European Commercial Aircraft before the Airbus A320." doi: 10.1002/9781119505433(2018), 1–30.
[14] Ijaz, S., Hamayun, M.T., Anwaar, H., Yan, L. and Li, M.K. "LPV modeling and tracking control of dissimilar redundant actuation system for civil aircraft, Int. J. Control Autom. Syst., 2019, **17**, pp 705–715.
[15] Kang, R., Jiao, Z., Shuai, W., Shang, Y. and Mare, J.C. The nonlinear accuracy model of electro-hydrostatic actuator, 2008 IEEE Conference on Robotics, Automation and Mechatronics, RAM 2008, 21–24 September 2008, Chengdu, China IEEE, 2008
[16] Röben, T. Hybrid actuation in primary flight control systems: a force-fight inhibiting system architecture, Rheinisch-Westfälischen Technischen Hochschule Aachen, [PhD Thesis], 2018.
[17] Kang, R., Jiao, Z., Wang, S. and Chen, L. Design and simulation of electro-hydrostatic actuator with a built-in power regulator, *Chinese J. Aeronaut.*, 2009, **22**, (6), pp 700–706.
[18] Kuznetsov, V.E., Khanh, N.D. and Lukichev, A.N. System for synchronizing forces of dissimilar flight control actuators with a common controller, 2020 XXIII International Conference on Soft Computing and Measurements (SCM), 2020.
[19] Li, Z., Shang, Y., Jiao, Z., Lin, Y., Wu, S. and Li, X. Analysis of the dynamic performance of an electro-hydrostatic actuator and improvement methods, *Chinese J. Aeronaut.*, 2018, **31**, pp 2312–2320.
[20] Bauer, G. *Ölhydraulik*. Springer, 2011, Berlin, Germany.
[21] Fesenmayr, J. Calculation of the volumetric and mechanical pump losses based on the A380 pump test results, Internal doc., Liebherr-Aerospace, 2004.
[22] Ren, G., Esfandiari, M., Song, J. and Sepehri, N. "Position control of an electro-hydrostatic actuator with tolerance to internal leakage," *IEEE Trans. Control Syst. Technol.*, 2016, **24**, (6), pp 2224–2232.
[23] Liang, T., Zhang, Y. and Wang, H. Fly by wire actuation system modeling and force fight equalization research, *J. Northwest. Polytech. Univ.*, 2020, **38**, (3), pp 643–648.
[24] AIR4253: Description of Actuation Systems for Aircraft With Fly-By-Wire Flight Control Systems - SAE International, 2021.
[25] Chen, Y., Tian, J., Wang, X., et al. "*Electrical Flight Control System Development and Certification for Regional Aircraft*," Shang Hai Jiao Tong University Press, ShangHai, China, 2019, pp 205–208.

Cite this article: Li D.W., Lin M.X. and Tian L. (2022). Research and modeling of force fighting equalisation for aircraft rudder's triple active actuation system. *The Aeronautical Journal*, **126**, 1801–1814. https://doi.org/10.1017/aer.2022.21